# Method for introducing bias magnetization in ungaped cores

*"The Saturation-Gap"*

Aguilar, Andres Revilla; Munk-Nielsen, Stig

*Published in:*
Proceedings of the 29th Annual IEEE Applied Power Electronics Conference and Exposition, APEC 2014.

*DOI (link to publication from Publisher):*
10.1109/APEC.2014.6803387

*Publication date:*
2014

*Document Version*
Early version, also known as pre-print

# Method for introducing bias magnetization in ungaped cores: “The Saturation-Gap”

*Andrés Revilla Aguilar and Stig Munk-Nielsen*
Energy Technology dept. Aalborg University
Aalborg, Denmark

***Abstract*— The use of permanent magnets for bias magnetization is a known technique to increase the energy storage capability in DC inductors, resulting in a size reduction or increased current rating. This paper presents a brief introduction on the different permanent magnet inductor’s configurations found in scientific literature. A new biasing configuration: *The Saturation-Gap*, will also be presented, simulated and experimentally tested.**

## I. INTRODUCTION

The use of air gaps in magnetic cores is a known technique, used to increase the saturation current and therefore the energy storage capability of the inductor. Another more recently develop technique combines air gaps with the use of permanent magnets for introducing an opposing bias flux in order to extend the saturation flux limit of DC inductors.

The first designs of biased DC inductors consisted of a permanent magnet inserted in the air gap [1][2]. This configuration can effectively produce a certain amount of bias flux in the inductor. The biasing will increase the saturation limit of the inductor and it will give the possibility of size reduction or improve the energy efficiency. On the other hand there are a number of limitations and drawbacks inherent to this configuration. The flux produced by the coil is passing through the permanent magnet itself, producing eddy currents and demagnetization effects. Another limitation of this configuration is related to the maximum amount of bias flux introduced by the permanent magnet. Since the maximum area cross section of the magnet must be equal or smaller than the area cross section of the core, the maximum bias flux will be limited by the flux density of the permanent magnet material.

More recent designs of biased inductors presents permanent magnets in the vicinity of the air gaps [3][4]. In these configurations the permanent magnets are outside the flux path of the coil, avoiding demagnetization effects and allowing the magnet size to be independent from air-gap dimensions. On the other hand they require non-standardized cores with specially designed shapes.

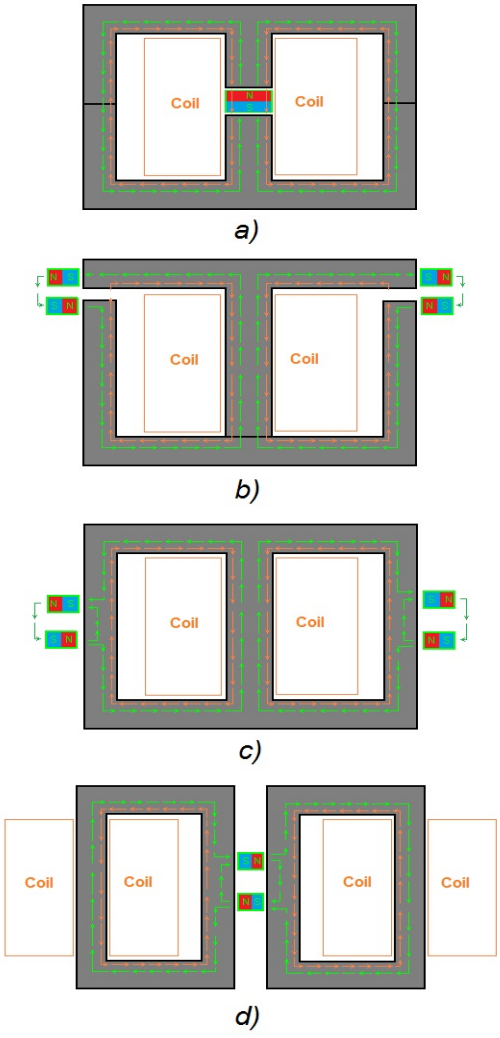


Fig. 1. Permanent magnet inductor configurations: *a)* Magnet inside air-gap, *b)* Magnets in the vicinity of air-gaps, *c)* Saturation-gap, *d)* Optimized saturation-gap. Red and green vectors represent coil and magnets flux respectively.

This paper presents a new core-magnet configuration consisting of external permanent magnets and standardized magnetic cores with no air gaps. The function of the permanent magnets in this configuration will be a twofold: to produce saturation in a localized segment of the core which will behave as a virtual air gap (*saturation-gap*) and to create a biasing flux in the rest of the core.

Fig.1. shows the core and magnets configurations of the previous mentioned strategies. The red and green arrows represent the coil and the magnet fluxes respectively. The portions of the core where the fluxes run in opposite directions are indicative of magnetic biasing; the smaller sections of the core where the fluxes run in the same direction are the saturation-gap regions.

The saturation-gap biasing concept has been experimentally tested on a EE30 ferrite core and Neodymium magnets arranged as in Fig.1.c). This configuration can introduce a 100% bias flux and increase the saturation current to double as compared with the same core with an standard air gap. Iron laminations cores have 3 to 4 times higher saturation flux limit than ferrite. The required bias flux from the magnet is equivalently increased. The configuration shown in Fig.1.d) can be used to optimize the required magnet size.

The following section II will present a simulation analysis of the saturation-gap concept using a magnetic equivalent circuit (MEC) approach. Section III will show empirical measurements performed on a EE30 ferrite core inductor and test it in a practical application operating as a flyback transformer. Finally, the conclusions and further work will be introduced in section IV.

## II. SIMULATION ANALISYS

The MEC model of the physically build inductor was simulated using LTspice software. In the present analysis we used a 2D matrix of 1 mm length reluctance elements to simulate the EE30 ferrite grade N87 core. The reluctance of each element is simulated by a non-linear resistor. The resistor´s V vs I values are introduced as a look-up table with the data found on the core specifications [8]. The same core model has been used in two different configurations: with 4mm air-gap in each leg; and without air-gap and with 5mm side cube shape magnets. Both models include a 40 turn winding represented as a flux (current) source which is related to the electrical winding in the model as in [7]. The magnet is model as an *mmf* (voltage) source with a series reluctance $R_m$. A parallel reluctance $R_{fring}$ is inserted to account for fringing flux [2]. Each 5x5x5 mm magnet is simulated as 5 magnets in parallel in order to match the 1mm resolution of the core reluctance model. Fig.2. presents the MEC models of the standard EE30 core with 4 mm air-gaps and with the saturation-gap configuration shown in Fig. 1.c)

The following formulas were used to calculate the related MEC parameters:

$$mmf = H_c l_m$$

$$R_m = \frac{l_m}{\mu_0 A_m}$$

$$R_{fring} = 2\,R_m$$

$$R_g = \frac{l_g}{\mu_0 A_g}$$

Where $R_g$ is the reluctance of the air-gaps, $H_c$ = *800KA/m* is the coercive force of the used Neodymium magnets, $A_m$ = *7 mm*$^2$ is the area cross section of each magnet segment, $l_m$ = *5 mm* is the length of the magnets, $l_g$ = *0.4 mm* is the length of the air-gaps, $A_g$ = *56 mm*$^2$ is the area of the central air-gap and *40mm*$^2$ the area of the side air-gap and $\mu_0$ is the permeability of vacuum. The air reluctance between the poles of the magnets facing away from the core are simulated as $R_g$ with $l_g$ = *2mm* and $A_c = A_m$.

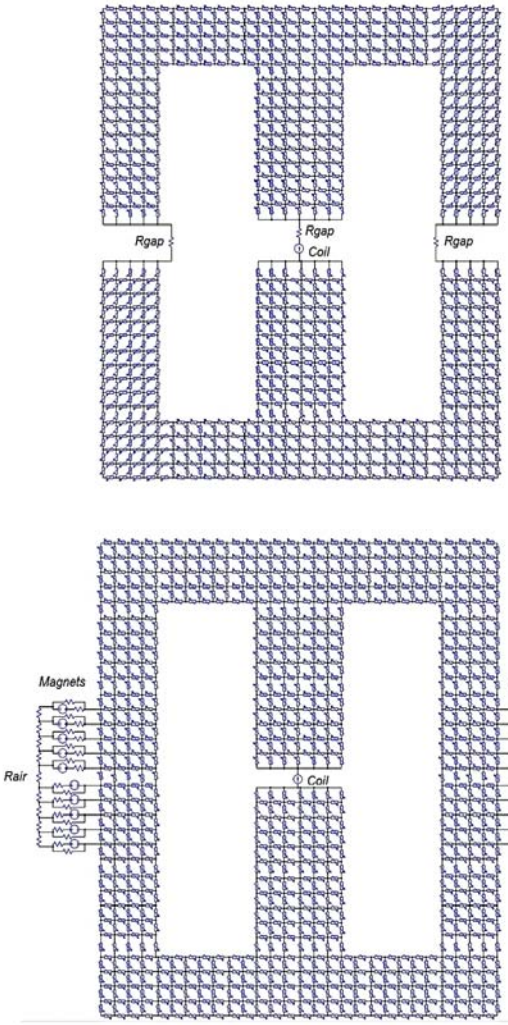


Fig. 2. MEC models. Top: EE30 core with 4mm air-gaps. Bottom: EE30 core with no gaps and with magnets in saturation-gap configuration. Core model is a 2D matrix with 1mm resolution, of characteristic N87 ferrite non-linear reluctance. Magnet model is a linear *mmf* source with series reluctance $R_m$ and parallel fringing reluctance $R_{fring}$. $R_{gap}$ and $R_{air}$ are standard lineal reluctances.

Fig. 3. shows the inductance versus current (LvsI) characteristic of each model obtained from the simulation results.

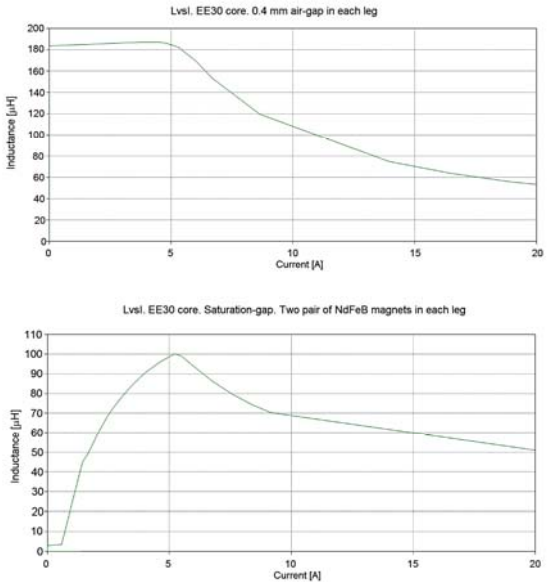


Fig. 3. Inductance versus Current results. Top: Standard EE30 ferrite core with 0.4 mm air-gap in each leg. Bottom: EE30 core with no air-gaps and saturation-gap.

The top plot in Fig.3. represents the expected LvsI curve of an standard inductor. The inductance has a constant value (180 uH approx.) in the nominal current region and it drops for currents higher to the saturation limit (5A approx.). The bottom plot presents the calculated LvsI of the saturation-gap configuration. The inductance value at 0 current is very low and gradually increases with the current. This is an indication of the presence of bias flux reaching to the negative saturation value of the core. The maximum inductance value appears at 5A and it is decreasing at higher currents at a slower rate compared with the standard non-biased core. The shapes of the obtained curves can serve as a rough indication of the biasing possibilities. On the other hand the specific obtained values differ greatly from the actual measurements and the proposed model results insufficiently accurate. A more detailed model considering the non-lineal effects of the permanent magnets would be needed.

## III. EXPERIMENTAL ANALISYS

The Saturation-Gap concept has been practically implemented and tested in a flyback converter. The used core is a EE30 of ferrite grade N87. The primary winding contains 40 turns and the secondary 80 turns. The same core and bobbin has been used in the tests with three different magnets or gap configurations:

- 1st EE30 core with 0.4 mm gap in both central and side legs. (Equivalent series gap is 0.8 mm.)
- 2nd EE30 core with no gap and 2 magnets in each leg.
- 3rd EE30 core with no gap and 3 magnets in each leg.

The magnets are placed in the side legs as shown in Fig. 1.c). Each leg presents 3 surfaces available for placing magnets. The used magnets are cubic shape with 5 mm side NdFeB with Br = 1.2 T.

Two different tests have been done in order to verify the theoretical possibilities of the biasing with the saturation-gap technique. The first test consists of the inductance versus current measurements of the inductor (LvsI). For the second test, a practical application consisting of a flyback converter was implemented.

### *A. Inductor Measurements*

The inductor characteristic of three configurations was measured using a Wayne Kerr magnetic analyzer at the 40 turns winding. The measurement was performed with *1V AC* stimuli at *8 kHz* and for a range of bias current. The analyzer measures the impedance and the phase angle and from these derives the inductance and the equivalent series resistance (ESR). The ESR value is compound with copper loses and core loses. The measured DC winding resistance is *27mOhm*.

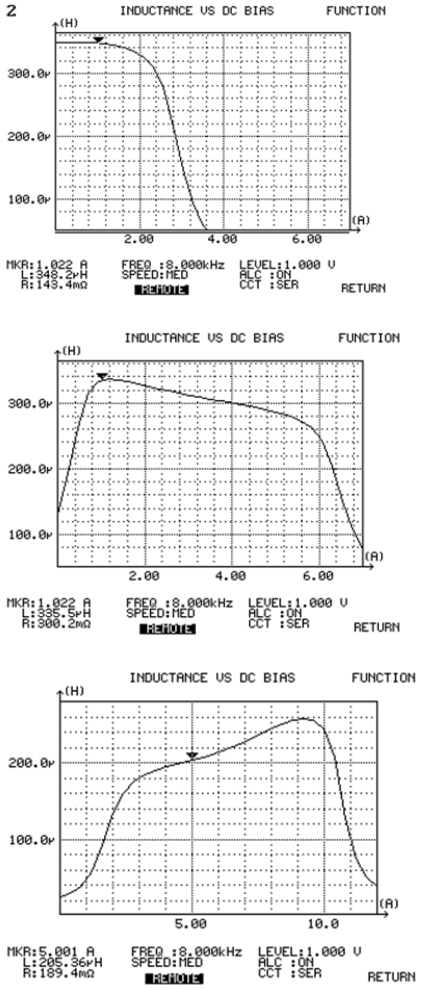


Fig. 4. Inductance vs Current measurement results. Top: Standard EE30 core with 0.4 mm air-gaps. Middle: Saturation-gap with EE30 core and 2 pairs of magnets in each leg. Bottom: Saturation-gap with EE30 core and 3 pairs of magnets in each leg. Measured with Wayne Kerr 3260B Magnetic Analyzer and 3265B bias unit.

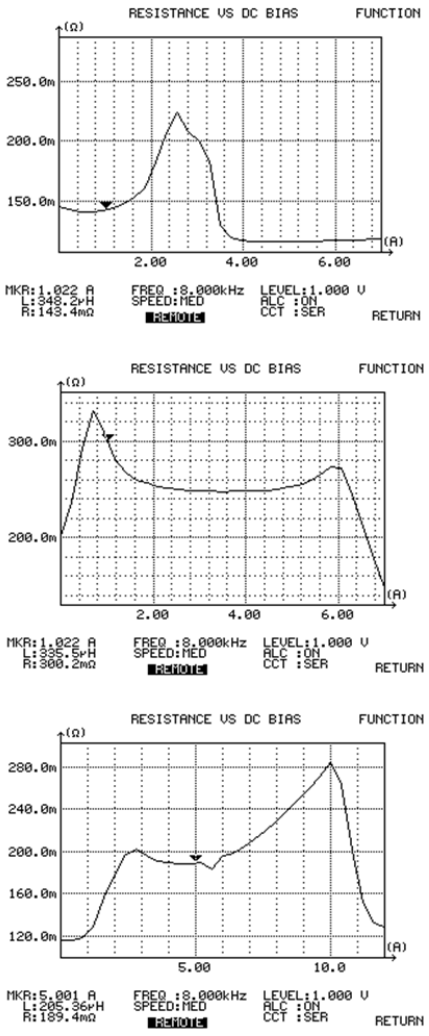


Fig. 5. Equivalent Series Resistance vs Current measurement results. Top: Standard EE30 core with 0.4 mm air-gaps. Middle: Saturation-gap with EE30 core and 2 pairs of magnets in each leg. Bottom: Saturation-gap with EE30 core and 3 pairs of magnets in each leg. Measured with Wayne Kerr 3260B Magnetic Analyzer and 3265B bias unit.

Fig.4. shows the obtained LvsI curves of the three configurations. The configuration with air-gaps presents the common LvsI profile with an inductor with a constant inductance in the nominal current region of *340 μH* and a roll-off at the saturation current approximately *2A*. The second and third configurations present a more particular LvsI profile. The nominal inductance region has been displaced to higher bias current levels, doubling the DC saturation current or displacing it even further. At the 0 current points the biased inductors presents a lower inductance value, indicative of the biasing flux is reaching the negative saturation of the core. The inductance in the nominal current range is also not constant but presents an ascending or descending slope in function of the bias current. These variations are due to the dynamically variable virtual air-gap produced by the saturation-gap region. These arrangements can be engineered to provide a specific LvsI profile which different inductor applications may benefit from.

Fig.5. presents the ESRvsI curves obtained from the mentioned measurements. The ERS values in the nominal inductance regions for the three configurations are representative of the core and magnet loses. At saturation current levels where the inductor impedance has drop to a small value, the measurement resolution is significantly low and the unexpectedly high values found may not be accurate. It can be noticed an increase in the core loses when using the saturation-gap technique. The same measurement performed at higher frequencies results in considerable increase in the losses of the 2nd and 3rd configurations. Interestingly, the losses of the 3rd configuration are lower than the 2nd while having more magnets and higher bias flux.

### *B. Flyback Converter Test*

The three configurations, performing as a flyback transformer were tested. The input voltage was initially set at 13v and was increased in steps until saturation was reach. The output load was adjusted in order to get an output voltage equal to four times that of the input. Fig. 6. shows a table with the measured input and output power and efficiency values for each configuration. Additionally, a plot presenting the converter efficiency in function of its output power is presented.

**Flyback Test. Frequency 8kHz. Duty cycle 70%**

| | | | Gap: 0.8mm No Mag | | | No Gap 4 Magnets | | | No Gap 6 Magnets | | |
|---|---|---|---|---|---|---|---|---|---|---|---|
| Ø [uVb] | Vi | Vo = 4*Vi | Pi [w] | Po [w] | Eff [%] | Pi [w] | Po [w] | Eff [%] | Pi [w] | Po [w] | Eff [%] |
| 28.4 | 13 | 52 | 15 | 12.5 | 83.3 | 10 | 8.7 | 87.0 | 20 | 17 | 85.0 |
| 30.6 | 14 | 56 | 17 | 14.1 | 82.9 | 12.3 | 10.7 | 87.0 | 23 | 19.6 | 85.2 |
| 32.8 | 15 | 60 | 20.4 | 16.6 | 81.4 | 14.4 | 12.5 | 86.8 | 26.5 | 22.5 | 84.9 |
| 35.0 | 16 | 64 | 25 | 19.5 | 78.0 | 16.4 | 14.2 | 86.6 | 30 | 25.5 | 85.0 |
| 37.2 | 17 | 68 | 33.5 | 22.8 | 68.1 | 19 | 16.5 | 86.8 | 34 | 28.7 | 84.4 |
| 38.3 | 17.5 | 70 | 55 | 28 | 50.9 | 20.3 | 17.6 | 86.7 | 35 | 29.6 | 84.6 |
| 43.8 | 20 | 80 | | | | 27 | 23.3 | 86.3 | 44 | 36.7 | 83.4 |
| 45.9 | 21 | 84 | | | | 31 | 26.4 | 85.2 | 47 | 39.2 | 83.4 |
| 48.1 | 22 | 88 | | | | 35.3 | 29.5 | 83.6 | 52 | 43 | 82.7 |
| 49.2 | 22.5 | 90 | | | | 36 | 30 | 83.3 | 54.6 | 45 | 82.4 |
| 54.7 | 25 | 100 | | | | 65 | 43 | 66.2 | 65 | 53.5 | 82.3 |
| 60.2 | 27.5 | 110 | | | | | | | 80 | 65 | 81.3 |
| 65.6 | 30 | 120 | | | | | | | 91 | 70 | 76.9 |

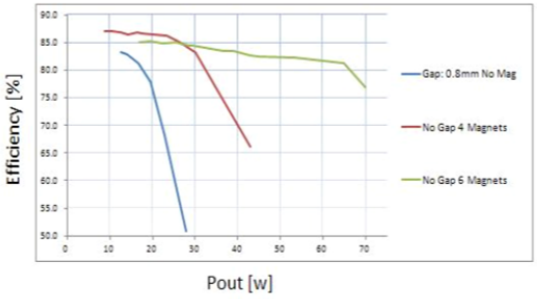


Fig. 6. Flayback transformer test. 40 turns primary winding, 80 turns secondary winding. EE30 Core in three different configurations: 0.4 mm air-gaps in each leg; Saturation-gap with EE30 core and 2 pairs of magnets in each leg; and Saturation-gap with EE30 core and 3 pairs of magnets in each leg. Data measured empirically.

It can be shown that the output power of the converter can be increased up to three times while having and equivalent efficiency. It is also noticeable that the efficiency of the 2nd configuration is higher than the 3rd configuration. This seems contra intuitive since the measured ESR values were also

higher. It must be of consideration that the measured values were tested using a DC bias current level and a small AC signal, while the flyback test is running in discontinuous mode having bigger current variations. In the following section IV a more in depth interpretation of the experimental data and the possible loss mechanisms involved when using the saturation gap will be given.

## IV. Conclusions and Further Work

The Saturation-Gap biasing configuration has been presented and experimentally tested. The output power rating of the tested inductor has been increased up to three times while having and equivalent efficiency compared to standard air-gap configuration.

The proposed MEC analysis can simulate some simple aspects of the saturation gap technique; on the other hand the simulated results deviate greatly from the empirical measurements. The dynamical variation of reluctance at the saturation-gap section is a complex function of the current and magnet flux. This section of the core will be operating in the most non-linear region of its BH loop. It is also know that the flux produce by a permanent magnet will present non-lineal variations in function of the reluctance around its flux path [5]. A more precise model including the permanent magnet non-linearity or a finite element model (FEM) will be required as further work.

The measured data can provide some indications of the possible loss mechanisms actuating in the saturation-gap arrangement. Core loses in standard inductors can be subdivided in two different types: eddy currents and hysteresis [9]. Eddy currents are produced in the magnetic core material, induced by the variations in flux, both in a macroscopic and microscopic scale (Barkhausen effect). Hysteresis loses are produced by friction, magnetostriction and delays in the dipoles and domain rotations within the crystalline structure of the core.

The presence of the permanent magnet flux will introduce an additional tension in the domain alignment reaching and equilibrium point different from that of the core alone. This mechanism could increase or even decrease the hysteresis loses of a given core. It is interesting to notice that the measured losses were lower in the configuration having a higher bias flux and accordingly higher tension within the dipoles and domains.

The important increase in core losses with frequency seems to indicate the presence of eddy currents. This is unexpected since the magnet is placed outside the coil's flux path. A similar eddy current mechanism seems to happen in the magnets. These eddy currents would not be directly induced by the variations in coil's flux, but by the internal variations of the flux produced by the permanent magnets themselves. The fluctuations of the flux from a permanent magnet are due to the variations in the reluctance of its magnetic path. This seems to correspond to the measured data since the higher losses are present at the saturation regions where the reluctance of the core is rapidly changing. The use of high resistivity magnets would help to minimize this loss mechanism.

The analysis of the possible design strategies for minimizing each of these loss mechanisms will be the focus for further work.

## References


[1] Teruhiko Fujiwara and Hatsuo Matsumoto. "A New Downsized Large Current Choke Coil with Magnet Bias Method". Telecommunications Energy Conference, 2003. INTELEC ´03. The 25th International. 23 October 2003. IEEE, pp. 416-420.

[2] Rafal Wrobel, Neville McNeill and Phil H. Mellor. "Design of a High-Temperature Pre-Biased Line Choke for Power Electronics Applications". Power Electronics Specialists Conference, 2008. PESC 2008. IEEE, pp 3171 – 3177.

[3] G.M. Shane and S.D. Sudhoff. "Permanent Magnet Inductor Design". Electric Ship Technologies Symposium, 2011 IEEE, pp. 330-333, April 10-13, 2011.

[4] G.M. Shane and S.D. Sudhoff. "Design and Optimization of Permanent Magnet Inductors". Applied Power Electronics Conference and Exposition (APEC), 27th Annual IEEE, pp 1770 – 1777.

[5] C.M. Andrews. "Understanding Permanent Magnets". TECH Notes Group Arnold.

[6] W.L. Soong. "BH Curve and Iron Loss Measurements for Magnetic Materials". Power Engineering Briefing Note Series. PEBN 5. 12 May 2008

[7] Stig Munk-Nielsen. "Experience with Spice teaching power electronics". Power Electronics and Applications, 2009. EPE ´09. 13th European Conference. IEEE, pp 1 – 8.

[8] EPCOS. "Ferrites and accessories. SIFERRIT material N87".

[9] John B. Goodenough. "Summary of losses in Magnetic Materials". IEEE Transactions on Magnetics. Vol. 38 NO 5 September 2002